CLNS 94/1298
CLEO 94-21

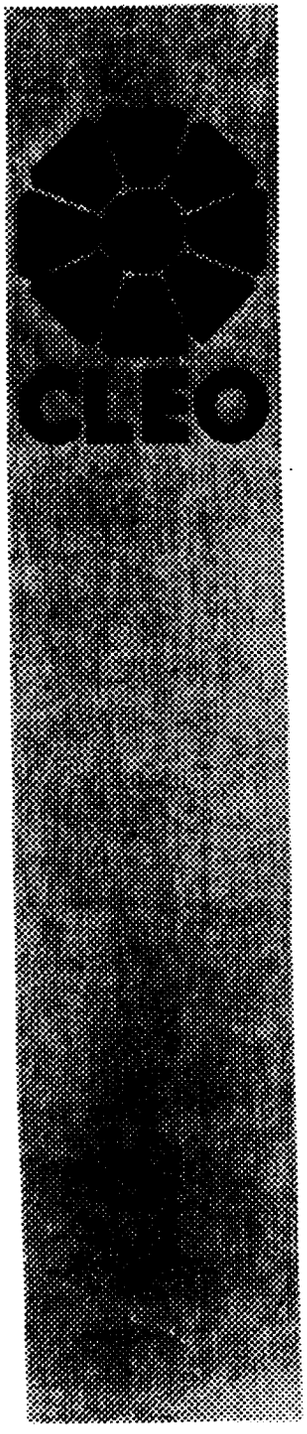

CALTECH UC-SAN DIEGO UC-SANTA BARBARA CARLETON COLORADO
CORNELL FLORIDA HARVARD ILLINOIS KANSAS MCGILL
MINNESOTA SUNY-ALBANY OHIO STATE OKLAHOMA PURDUE
ROCHESTER SOUTHERN-METHODIST SYRACUSE VANDERBILT VIRGINIA TECH

Observation of $D_1(2420)^+$ and $D_2^*(2460)^+$

CLNS 94/1298
CLEO 94-21
September 22, 1994

Observation of $D_1(2420)^+$ and $D_2^*(2460)^+$

T. Bergfeld,[1] B.I. Eisenstein,[1] G. Gollin,[1] B. Ong,[1] M. Palmer,[1] M. Selen,[1] J. J. Thaler,[1] K.W. Edwards,[2] M. Ogg,[2] A. Bellerive,[3] D.I. Britton,[3] E.R.F. Hyatt,[3] D.B. MacFarlane,[3] P.M. Patel,[3] B. Spaan,[3] A.J. Sadoff,[4] R. Ammar,[5] P. Baringer,[5] A. Bean,[5] D. Besson,[5] D. Coppage,[5] N. Copty,[5] R. Davis,[5] N. Hancock,[5] M. Kelly,[5] S. Kotov,[5] I. Kravchenko,[5] N. Kwak,[5] H. Lam,[5] Y. Kubota,[6] M. Lattery,[6] M. Momayezi,[6] J.K. Nelson,[6] S. Patton,[6] R. Poling,[6] V. Savinov,[6] S. Schrenk,[6] R. Wang,[6] M.S. Alam,[7] I.J. Kim,[7] Z. Ling,[7] A.H. Mahmood,[7] J.J. O'Neill,[7] H. Severini,[7] C.R. Sun,[7] F. Wappler,[7] G. Crawford,[8] C. M. Daubenmier,[8] R. Fulton,[8] D. Fujino,[8] K.K. Gan,[8] K. Honscheid,[8] H. Kagan,[8] R. Kass,[8] J. Lee,[8] R. Malchow,[8] M. Sung,[8] C. White,[8] M.M. Zoeller,[8] F. Butler,[9] X. Fu,[9] B. Nemati,[9] W.R. Ross,[9] P. Skubic,[9] M. Wood,[9] M. Bishai,[10] J. Fast,[10] E. Gerndt,[10] J.W. Hinson,[10] R.L. McIlwain,[10] T. Miao,[10] D.H. Miller,[10] M. Modesitt,[10] D. Payne,[10] E.I. Shibata,[10] I.P.J. Shipsey,[10] P.N. Wang,[10] M. Battle,[11] J. Ernst,[11] L. Gibbons,[11] Y. Kwon,[11] S. Roberts,[11] E.H. Thorndike,[11] C.H. Wang,[11] J. Dominick,[12] M. Lambrecht,[12] S. Sanghera,[12] V. Shelkov,[12] T. Skwarnicki,[12] R. Stroynowski,[12] I. Volobouev,[12] G. Wei,[12] P. Zadorozhny,[12] M. Artuso,[13] M. Gao,[13] M. Goldberg,[13] D. He,[13] N. Horwitz,[13] G.C. Moneti,[13] R. Mountain,[13] F. Muheim,[13] Y. Mukhin,[13] S. Playfer,[13] Y. Rozen,[13] S. Stone,[13] X. Xing,[13] G. Zhu,[13] J. Bartelt,[14] S.E. Csorna,[14] Z. Egyed,[14] V. Jain,[14] D. Gibaut,[15] K. Kinoshita,[15] P. Pomianowski,[15] B. Barish,[16] M. Chadha,[16] S. Chan,[16] D.F. Cowen,[16] G. Eigen,[16] J.S. Miller,[16] C. O'Grady,[16] J. Urheim,[16] A.J. Weinstein,[16] M. Athanas,[17] W. Brower,[17] G. Masek,[17] H.P. Paar,[17] J. Gronberg,[18] R. Kutschke,[18] S. Menary,[18] R.J. Morrison,[18] S. Nakanishi,[18] H.N. Nelson,[18] T.K. Nelson,[18] C. Qiao,[18] J.D. Richman,[18] A. Ryd,[18] D. Sperka,[18] H. Tajima,[18] M.S. Witherell,[18] R. Balest,[19] K. Cho,[19] W.T. Ford,[19] D.R. Johnson,[19] K. Lingel,[19] M. Lohner,[19] P. Rankin,[19] J.G. Smith,[19] J.P. Alexander,[20] C. Bebek,[20] K. Berkelman,[20] K. Bloom,[20] T.E. Browder,[20*] D.G. Cassel,[20] H.A. Cho,[20] D.M. Coffman,[20] D.S. Crowcroft,[20] P.S. Drell,[20] D.J. Dumas,[20] R. Ehrlich,[20] P. Gaidarev,[20] M. Garcia-Sciveres,[20] B. Geiser,[20] B. Gittelman,[20] S.W. Gray,[20] D.L. Hartill,[20] B.K. Heltsley,[20] S. Henderson,[20] C.D. Jones,[20] S.L. Jones,[20] J. Kandaswamy,[20] N. Katayama,[20] P.C. Kim,[20] D.L. Kreinick,[20] G.S. Ludwig,[20] J. Masui,[20] J. Mevissen,[20] N.B. Mistry,[20] C.R. Ng,[20] E. Nordberg,[20] J.R. Patterson,[20] D. Peterson,[20] D. Riley,[20] S. Salman,[20] M. Sapper,[20] F. Würthwein,[20] P. Avery,[21] A. Freyberger,[21] J. Rodriguez,[21] S. Yang,[21] J. Yelton,[21] D. Cinabro,[22] T. Liu,[22] M. Saulnier,[22] R. Wilson,[22] and H. Yamamoto[22]

(CLEO Collaboration)

[1] *University of Illinois, Champaign-Urbana, Illinois, 61801*
[2] *Carleton University, Ottawa, Ontario K1S 5B6 and the Institute of Particle Physics, Canada*
[3] *McGill University, Montréal, Québec H3A 2T8 and the Institute of Particle Physics, Canada*
[4] *Ithaca College, Ithaca, New York 14850*
[5] *University of Kansas, Lawrence, Kansas 66045*
[6] *University of Minnesota, Minneapolis, Minnesota 55455*
[7] *State University of New York at Albany, Albany, New York 12222*
[8] *Ohio State University, Columbus, Ohio, 43210*
[9] *University of Oklahoma, Norman, Oklahoma 73019*
[10] *Purdue University, West Lafayette, Indiana 47907*
[11] *University of Rochester, Rochester, New York 14627*
[12] *Southern Methodist University, Dallas, Texas 75275*
[13] *Syracuse University, Syracuse, New York 13244*
[14] *Vanderbilt University, Nashville, Tennessee 37235*
[15] *Virginia Polytechnic Institute and State University, Blacksburg, Virginia, 24061*
[16] *California Institute of Technology, Pasadena, California 91125*
[17] *University of California, San Diego, La Jolla, California 92093*
[18] *University of California, Santa Barbara, California 93106*
[19] *University of Colorado, Boulder, Colorado 80309-0390*
[20] *Cornell University, Ithaca, New York 14853*
[21] *University of Florida, Gainesville, Florida 32611*
[22] *Harvard University, Cambridge, Massachusetts 02138*

Abstract

Using the CLEO II detector at CESR, we have observed two charmed states, where the higher mass state decays to $D^0\pi^+$ and to $D^{*0}\pi^+$, while the lower mass state decays to $D^{*0}\pi^+$, but not to $D^0\pi^+$. The masses and widths were measured to be $2425 \pm 2 \pm 2$ MeV/c^2 and 26^{+8+4}_{-7-4} MeV/c^2 for the lower mass state, and $2463 \pm 3 \pm 3$ MeV/c^2 and 27^{+11+5}_{-8-5} MeV/c^2 for the higher mass state. Properties of these states, including their decay angular distributions and spin-parity assignments have been studied. The results of this analysis support the identification of these states as the charged $L = 1$ $D_1(2420)^+$ and $D_2^*(2460)^+$, respectively. The isospin mass splittings between these states and their neutral partners have also been measured. This is the first full reconstruction of any decay mode of the $D_1(2420)^+$ and the first observation of the decay of $D_2^*(2460)^+$ to $D^{*0}\pi^+$.

---

*Permanent address: University of Hawaii at Manoa

I. INTRODUCTION

The D_J mesons consist of one charmed quark (Q) and one light quark ($\bar{q}$) with relative orbital angular momentum L. When $L = 1$, there are four states with spin-parity $J^P = 0^+$, 1^+, 1^+ and 2^+. In the notation introduced by the Particle Data Group [1], these states are labeled D_0^*, D_1 for both 1^+ states, and D_2^* respectively.

Parity and angular momentum conservation place restrictions on the strong decays of these D_J states to $D\pi$ and $D^*\pi$: the 0^+ state can decay only to $D\pi$ through S-wave decay, either 1^+ state can decay to $D^*\pi$ through S-wave or D-wave decays, and the 2^+ state can decay to both $D\pi$ and $D^*\pi$ only through D-wave decays.

In the decay chain $D_J \to D^*\pi$ with $D^* \to D\pi$, the helicity angle distribution of the D^* can be used to analyze the spin of the parent D_J. The helicity angle, denoted by α, is defined as the angle between the π^+ from the decay $D_J^+ \to D^{*0}\pi^+$ and the π^0 from the decay $D^{*0} \to D^0\pi^0$, both measured in the D^{*0} rest frame. Regardless of the initial polarization of the D_J states, the predicted helicity angle distributions are:

$$\frac{dN}{d\cos\alpha} \propto \begin{cases} \sin^2\alpha & (2^+ \text{ state}) \\ 1 & (\text{pure S-wave } 1^+ \text{ state}) \\ 1 + 3\cos^2\alpha & (\text{pure D-wave } 1^+ \text{ state}) \end{cases} \quad (1)$$

Two D_J^0 states, the $D_1(2420)^0$ and the $D_2^*(2460)^0$, have been observed by ARGUS [2–4], E691 [5], CLEO 1.5 [6], E687 [7], and CLEO II [8]. However, their isospin partners are not so well established. The $D_2^*(2460)^+$ has only been observed, by ARGUS [9] and E687 [7], in its decay to $D^0\pi^+$. Indirect evidence for the $D_1(2420)^+$ † was obtained by E691 [5]. They observed a broad enhancement in the $D^0\pi^+$ spectrum which they attributed to the decay $D_1^+ \to D^{*0}\pi^+$, and the subsequent decay, $D^{*0} \to D^0\pi^0$ or $D^0\gamma$ with the π^0's or γ's being undetected. No previous experiment has been able to reconstruct fully a $D_1(2420)^+$ candidate or has been able to observe both the $D_1(2420)^+$ and the $D_2^*(2460)^+$ states.

The large data sample collected with the CLEO II detector, together with its capability to make precision measurements of both charged and neutral particles, allows us to identify two of the D_J^+ states and to measure their corresponding angular distributions. Moreover, the isospin mass splittings between the charged and neutral states can be measured.

II. HEAVY QUARK EFFECTIVE THEORY

Heavy Quark Effective Theory (HQET) predicts the presence of an approximate flavor-spin symmetry for hadrons containing one heavy quark ($m_Q \gg \Lambda_{QCD}$) [10,11]. In the limit $m_Q \to \infty$, the mesons are described by S_Q (spin of the heavy quark), $j = S_q + L$ (total angular momentum of the light quark), and $J = j + S_Q$ (total angular momentum). The mesons with $L = 1$ are then arranged in 2 doublets as shown in Table I.

In this limit, the $j = 3/2$ mesons are predicted to decay exclusively in a D-wave, while the $j = 1/2$ mesons decay only in an S-wave [10,12]. Mesons whose favored decay is D-wave

†The Particle Data Group [1] refers to this state as the $D_J(2440)^+$.

are predicted to be relatively narrow (widths of tens of MeV/c^2), while those of the other doublet are predicted to be quite broad (widths of hundreds of MeV/c^2). Models [12-14] predict the ratio of the branching fractions, $B(D_2^* \to D\pi)/B(D_2^* \to D^*\pi)$, to lie in the range from 1.5 to 3.0.

Because of the finite mass of the c quark, the $P_1^{(3/2)} \to D^*\pi$ decay may also proceed via an S-wave. In this case, HQET predicts that this S-wave amplitude is small compared with typical S-wave amplitudes, but it makes no prediction for the relative magnitudes of the S-wave and D-wave amplitudes [10]. On the other hand, the presence of an S-wave partial width has been considered in potential models [13], and its contribution, expressed in terms of $\Gamma_S/(\Gamma_S + \Gamma_D)$, where Γ_S is the S-wave partial width and Γ_D is the D-wave partial width, was predicted to lie between 0.2 and 0.7. These general features were observed in an earlier study, by the CLEO II collaboration, of the decay $D_1(2420)^0 \to D^{*+}\pi^-$ [8].

III. DATA SAMPLE AND EVENT SELECTION

The data used in this analysis were selected from hadronic events produced in e^+e^- annihilations at CESR and collected with the CLEO II detector. The CLEO II detector measures both neutral and charged particles with excellent resolution and efficiency. A detailed description of the detector can be found elsewhere [15].

The center-of-mass energies used in this analysis were at the mass of the $\Upsilon(4S)$, $E_{CM.} = 10.580$ GeV, and in the nearby continuum. The data corresponds to an integrated luminosity of 2.37 fb^{-1}. We selected hadronic events that have a minimum of three charged tracks, a total visible energy greater than 15% of the center-of-mass energy (this reduced contamination from two-photon interactions and beam-gas events), and a primary vertex within ± 2 cm in the r-ϕ plane (perpendicular to the beam) and ± 5 cm in the z-direction (the beam direction) of the nominal interaction point.

Each track was required to have an impact parameter in the r-ϕ plane of less than 5 mm and to have a distance of closest approach in the z-direction of less than 5 cm, both with respect to the interaction point. All charged tracks were also required to have dE/dx information. If available, time-of-flight information was also used.

When reconstructing π^0's, we used pairs of photons from the barrel region, $|\cos\theta| < 0.707$, where the energy resolution is best. The photons were required to have a minimum energy of 50 MeV and to be isolated from charged tracks. All π^0 candidates, whose invariant mass lay within 50 MeV/c^2 of the π^0 mass, were kinematically fit to the known π^0 mass [1] and, in addition, were required to have a momentum of at least 65 MeV/c.

IV. $D_J^+ \to D^0\pi^+$

To reconstruct $D_J^+ \to D^0\pi^+$ ‡, we first reconstructed the D^0 in the decay mode $K^-\pi^+$. The distribution of the decay angle, θ_K, defined as the angle between the direction of the

‡References in this paper to a specific state or decay will always imply that the charge-conjugate state or decay has also been included.

D^0 momentum in the lab and the direction of the K^- momentum in the D^0 rest frame, is expected to be flat for signal combinations. It showed, however, a large peak at $\cos\theta_K = 1$, due to spurious combinations of a forward K with a slow π. A cut of $\cos\theta_K < 0.8$ was accordingly applied. Since many D^0's come from D^* decays, we used only D^0 candidates which were not reconstructed daughters of a D^*. This was accomplished by combining each D^0 candidate with each remaining π^+ and π^0 in the event and requiring that, for every $D^0\pi$ combination, $M(D^0\pi^+) - M(D^0) \geq 150$ MeV/c^2 or $M(D^0\pi^0) - M(D^0) \geq 147$ MeV/c^2. Each D^0 candidate, surviving the cuts outlined above, was then combined with each remaining π^+ in the event. In order to reduce combinatorial background we applied a further cut of $x_p(D^0\pi^+) > 0.65$, where $x_p = p/p_{max}$ and $p_{max} = \sqrt{E^2_{beam} - M^2_{D^+_J}}$. We also studied the distribution of $\cos\theta_\pi$, where the decay angle, θ_π, is defined as the angle between the direction of the $D^0\pi^+$ momentum in the lab and the direction of the π^+ momentum in the $D^0\pi^+$ rest frame. This distribution is expected to be symmetric about zero for signal events, but the data showed a prominent peak at $\cos\theta_\pi = -1$. This peak is produced by combinations of the D^0 with the many slow π^+ tracks in an event. A cut of $\cos\theta_\pi > -0.3$ was applied to suppress this large background contribution. We then calculated the total probability, P_{tot}, of the candidate using the particle identification (dE/dx and time-of-flight) and the reconstructed D^0 mass. $P_{tot}(\chi^2_{tot}, N_{dof})$ is defined as the probability to observe $\chi^2 > \chi^2_{tot}$ for N_{dof} degrees of freedom. For signal events this distribution should be flat but due to background combinations a prominent peak was observed at $P_{tot} = 0$. In order to reduce this background we required $P_{tot} > 0.1$.

The spectrum of the mass-difference, $M(D^0\pi^+) - M(D^0)$, for all $D^0\pi^+$ combinations surviving the above cuts is shown in Fig. 1. This spectrum was fitted with a third-order Chebychev polynomial for the background and a Breit-Wigner resonance shape, convoluted with a Gaussian resolution function, for the signal. The σ of this Gaussian function was fixed to 4 MeV/c^2, as determined from Monte Carlo studies. The region from 390 to 440 MeV/c^2 was excluded from the fit because this region is populated by feed-down, caused by not reconstructing π^0's or γ's in some D^+_J decay chains, such as $D^+_J \to D^{*0}\pi^+$, with $D^{*0} \to D^0\pi^0$ or $D^0\gamma$. Our fit yielded 312^{+98}_{-79} signal events with a value $M(D^0\pi^+) - M(D^0) = 598 \pm 3 \pm 3$ MeV/c^2, which corresponds to a mass $M = 2463 \pm 3 \pm 3$ MeV/c^2, and an intrinsic width $\Gamma = 27^{+11+5}_{-\ 8-5}$ MeV/c^2. This state will be identified below as the $D^*_2(2460)^+$ state. The first error is statistical and the second error is systematic, which was estimated by varying the cuts, the background parameterization, and spin of the Breit-Wigner distribution used. Our results for the mass and width of this state, along with previous measurements, are listed in Table II.

V. $D^+_J \to D^{*0}\pi^+$

To reconstruct $D^+_J \to D^{*0}\pi^+$ we first reconstructed D^0's in the decay modes $K^-\pi^+$ and $K^-\pi^+\pi^0$. The D^{*0} candidates were reconstructed by combining each D^0 candidate with each remaining π^0 in the event. Each D^{*0} candidate was then combined with each remaining π^+ in the event. In order to reduce combinatorial background, a cut of $x_p(D^{*0}\pi^+) > 0.6$ and a cut of $\cos\theta_\pi > -0.7$ were applied. The decay angle, θ_π, is defined as the angle between the direction of the $D^{*0}\pi^+$ momentum in the lab and the direction of the π^+ momentum in the $D^{*0}\pi^+$ rest frame. The motivation for applying this cut is similar to that discussed

above in the analysis of the decay $D^+_J \to D^0\pi^+$. We calculated P_{tot} using the particle identification (dE/dx and time-of-flight), the D^0 mass, the π^0 mass, and the mass-difference $M(D^{*0}) - M(D^0)$. We required $P_{tot} > 0.1$.

The spectrum of the mass-difference, $M(D^{*0}\pi^+) - M(D^{*0})$, for all combinations passing the above cuts is shown in Fig. 2. The $D^*_2(2460)^+$ state appears as a shoulder on the high mass side of the more prominent low mass state. The latter will be identified below as the $D_1(2420)^+$ state. This spectrum was fitted with a fourth-order Chebychev polynomial for the background and two Breit-Wigner resonance shapes convoluted with Gaussian resolution functions for the signals. For each of these Gaussian functions we fixed $\sigma = 3$ MeV/c^2, as determined from Monte Carlo studies. The mass and width of one convoluted Breit-Wigner were constrained to the measured values obtained above from the decay $D^*_2(2460)^+ \to D^0\pi^+$, while the parameters of the other convoluted Breit-Wigner were left free. The fit yielded 204^{+61}_{-50} $D_1(2420)^+$ signal events and 115^{+41}_{-40} $D^*_2(2460)^+$ signal events. We also obtained from the fit $M(D^+_1) - M(D^{*0}) = 419^{+3}_{-2}$ MeV/c^2 and $\Gamma = 19^{+9}_{-7}$ MeV/c^2.

The difference in the expected $\cos\alpha$ distributions, outlined above, can be used to separate the two D^+_J states which decay to $D^{*0}\pi^+$. In order to determine the mass and width of the $D_1(2420)^+$ state and, at the same time, to improve the signal to background ratio, the $D^*_2(2460)^+$ state was suppressed by requiring $|\cos\alpha| > 0.8$. The $M(D^{*0}\pi^+) - M(D^{*0})$ spectrum for all combinations passing the above cuts with $|\cos\alpha| > 0.8$ is shown in Fig. 3. The prominent peak observed is due to the $D_1(2420)^+$ state, with the higher mass state clearly having been suppressed. The fitted values for the mass and width of the $D_1(2420)^+$ were obtained in two different ways. In the first method, the mass and width of the higher mass state were constrained to the values given above for the decay $D^*_2(2460)^+ \to D^0\pi^+$, while the parameters for the $D_1(2420)^+$ state were left free. For the suppressed $D^*_2(2460)^+$ state, we then obtained 0 ± 9 events. For the $D_1(2420)^+$ state, the fit yielded 146^{+33}_{-29} signal events, $M(D^+_1) - M(D^{*0}) = 418 \pm 2 \pm 2$ MeV/c^2, and $\Gamma = 26^{+8+4}_{-7-4}$ MeV/c^2, in good agreement with those obtained above. The measured mass-difference corresponds to a $D_1(2420)^+$ mass of $M = 2425 \pm 2 \pm 2$ MeV/c^2. The second error is systematic and was estimated by varying the cuts, the mass and width of the fixed state, the background parameterization, and the spin of the Breit-Wigner shapes used to describe the signals. In the second method, simultaneous fits were made to both the $M(D^0\pi^+) - M(D^0)$ and $M(D^{*0}\pi^+) - M(D^{*0})$ spectra shown in Fig. 1 and Fig. 3, with the constraint that the fitted mass and width of the $D^*_2(2460)^+$ be the same for both spectra. This approach yielded values for the mass and width of the $D_1(2420)^+$ state which were within 0.5 MeV/c^2 of those obtained with the first method.

A comparison of the $M(D^{*0}\pi^+) - M(D^{*0})$ spectra in Figs. 2 and 3 shows that the helicity angle cut, $|\cos\alpha| > 0.8$, not only strongly enhances the $D_1(2420)^+$ signal to background ratio but also suppresses the high mass shoulder from the $D^*_2(2460)^+$ state. We therefore report the values of the mass and width of the $D_1(2420)^+$ state to be those obtained from the fit to the spectrum with $|\cos\alpha| > 0.8$. These data and fit are shown in Fig. 3. The only previous evidence for the existence of the D^+_1 was obtained by E691 [5], as discussed above. They reported values of $M = 2443 \pm 7 \pm 5$ MeV/c^2 and $\Gamma = 41 \pm 19 \pm 8$ MeV/c^2.

VI. ISOSPIN MASS SPLITTINGS

In an earlier CLEO II study [8], the $D_2^*(2460)^0$ and $D_1(2420)^0$ states were identified as the neutral P-wave charmed mesons and their masses and widths were measured. The mass values obtained were $2465 \pm 3 \pm 3$ MeV/c^2 for the $D_2^*(2460)^0$ state and 2421^{+1+2}_{-2-2} MeV/c^2 for the $D_1(2420)^0$ state. From the data presented above, the mass splitting between the $D_2^*(2460)^+$ and the $D_2^*(2460)^0$ and that between the $D_1(2420)^+$ and the $D_1(2420)^0$ are, at most, only a few MeV/c^2, characteristic of mass splittings within isospin multiplets.

It is therefore natural to propose that the two charged states reported here are the isospin partners of the previously established neutral states. The near equality of the widths of the states within each proposed isospin doublet lends further support to this hypothesis.

We have accordingly extracted the isospin mass splittings, $M[D_2^*(2460)^+] - M[D_2^*(2460)^0]$ and $M[D_1(2420)^+] - M[D_1(2420)^0]$. Since the dominant systematic errors on the masses are due to the background shape, the individual errors were simply added in quadrature. The contribution to the systematic error from the uncertainty in the momentum scale of the charged tracks is negligible. These results are summarized in Table III, along with measurements from earlier experiments.

VII. HELICITY ANGLE DISTRIBUTIONS

We now attempt to determine the spins and parities of these D_J^+ states by investigating the helicity angle distributions in the decays $D_J^+ \to D^{*0}\pi^+$. The various spin-parity hypotheses and the corresponding helicity angle distributions, for the general case of D_J decays to $D^*\pi$, are listed in Table IV.

As discussed in the earlier CLEO II study [8], the dependence of the helicity angle distribution on the alignment of the D_J^+ may be removed by releasing the cut on $\cos\theta_\pi$. We therefore released the $\cos\theta_\pi$ cut and fitted the $M(D^{*0}\pi^+) - M(D^{*0})$ mass-difference spectra in four bins of $\cos\alpha$ from -1 to 1. The masses and widths of both states were fixed to our measured values given above. This yields the number of D_J^+ events in each $\cos\alpha$ bin. The normalized helicity angle distributions for the $D_2^*(2460)^+$ and $D_1(2420)^+$ states are shown in Fig. 4 and Fig. 5, respectively. The error assigned to the contents of each bin in these plots is only the statistical error, and does not contain a contribution from the uncertainty in the mass and width of the state being investigated. The shape of the $\cos\alpha$ distribution was found not to be significantly affected when the mass and width fixed in the fit were varied within their measured uncertainties.

Monte Carlo studies showed that, on the scale of our statistical errors, our efficiency is independent of the helicity angle and does not vary significantly over $\cos\theta_\pi$. We evaluated the χ^2 per degree of freedom (χ^2/N_{dof}), and confidence level (CL), for various hypotheses for the shape of these distributions. The results are listed in Table V.

The observation of the decay $D_2^*(2460)^+ \to D^0\pi^+$ restricts the $D_2^*(2460)^+$ to have natural spin-parity, $J^P = 0^+, 1^-, 2^+, \ldots$ In addition, the observation of the decay $D_2^*(2460)^+ \to D^{*0}\pi^+$ excludes $J^P = 0^+$. The remaining hypotheses will give a helicity angle distribution proportional to $\sin^2\alpha$, which is seen in Table V to be preferred. Mesons with $L > 1$ are expected to be highly suppressed in the fragmentation process, suggesting that only the $J^P = 1^-, 2^+$ hypotheses are acceptable for the $D_2(2460)^+$ state. We note that the

assignment $J^P = 1^-$ would imply that this state is a radial excitation of the D^{*+}. Such a state is expected [16], however, to have a mass about 180 MeV/c^2 higher than the state observed here, and this assignment is therefore unlikely. This leaves $J^P = 2^+$, as the most likely assignment for the $D_2^*(2460)^+$ state, consistent with the parallel analysis of the corresponding neutral state, $D_2^*(2460)^0$ [8].

We now investigate the decay of the $D_1(2420)^+$ state. The only observed decay mode is $D_1(2420)^+ \to D^{*0}\pi^+$, thus forbidding this state to have $J^P = 0^+$. The results, presented in Table V, show that the $\sin^2\alpha$ hypothesis is excluded at more than 99% CL. Referring to Table IV, this is seen to exclude the $D_1(2420)^+$ state from having the quantum numbers $J^P = 1^-, 2^+, 3^-, \ldots$, leaving the possible assignments, $J^P = 0^-, 1^+, 2^-, \ldots$ We recall that mesons with $L > 1$ are expected to be highly suppressed in the fragmentation process, suggesting that only the $J^P = 0^-, 1^+$ hypotheses are acceptable for the $D_1(2420)^+$ state. As seen in Table V, the $\cos^2\alpha$ hypothesis is acceptable, which allows the assignment, $J^P = 0^-$. However, this assignment would imply that this state is a radial excitation of the D^+. Such a state is expected [16] to have a mass about 150 MeV/c^2 higher than the state observed here and this assignment is therefore unlikely. This leaves the assignment $J^P = 1^+$ as the most probable for the $D_1(2420)^+$ state.

As discussed above, in the limit $m_Q \to \infty$, HQET predicts that the $P_1^{3/2}$ mesons undergo a pure D-wave decay. The resulting distribution would then have the form, $1 + 3\cos^2\alpha$. It is therefore of interest to calculate the CL for this hypothesis. The result is given in Table V. It is seen that this hypothesis gives a good description of the data.

The nature of the helicity angular distributions for these $D_J^+ \to D^{*0}\pi^+$ decays may also be investigated by fitting these distributions to the form $A(1 + B\cos^2\alpha)$ and constraining B to the physically allowed values from -1 to ∞. For the $D_2^*(2460)^+$ decay distribution, this gave the result, $B = -1.00^{+0.23}_{-0.00}$ with $\chi^2/N_{dof} = 1.3/2$ and a CL = 51.3%. For the $D_1(2420)^+$ decay distribution, this gave the result, $B = 3.55^{+5.26}_{-2.02}$ with $\chi^2/N_{dof} = 1.6/2$ and a CL = 44.9%.

The most likely assignments are, therefore, that the $D_2^*(2460)^+$ state has $J^P = 2^+$ and that the $D_1(2420)^+$ has $J^P = 1^+$. This supports the proposal that the $D_2^*(2460)^+$ and $D_1(2420)^+$ states should be identified as two of the charged P-wave charmed mesons. In the HQET picture, the observed narrow widths of these states suggest that they are the $P_2^{(3/2)}$ and $P_1^{(3/2)}$ ($j = 3/2$) $c\bar{d}$ doublet.

The conclusions from the analysis presented here of the angular distributions of the $D_2^*(2460)^+$ and $D_1(2420)^+$ decays are consistent with those from the parallel analysis of the $D_2^*(2460)^0$ and $D_1(2420)^0$ states [8]. These provide further evidence for identifying these states as the isospin partners of the $D_2^*(2460)^0$ and $D_1(2420)^0$ states.

Assuming that the $D_1(2420)^+$ does indeed have $J^P = 1^+$, both S-wave and D-wave amplitudes are allowed in its decay to $D^{*0}\pi^+$. The general form of the helicity angle distribution for the decay $D_1(2420)^+ \to D^{*0}\pi^+$ is then [8]:

$$\frac{1}{N}\frac{dN}{d\cos\alpha} = \frac{1}{2}\left\{\mathrm{R} + (1-\mathrm{R})\left[\frac{1+3\cos^2\alpha}{2}\right] + \sqrt{2\mathrm{R}(1-\mathrm{R})}\cos\varphi\left[1-3\cos^2\alpha\right]\right\}, \qquad (2)$$

where $\mathrm{R} = \Gamma_S/(\Gamma_S + \Gamma_D)$, Γ_S is the S-wave partial width, Γ_D is the D-wave partial width, and φ is the relative phase of the two amplitudes.

The hatched region in Fig. 6 shows the region of the R-cos φ plane which is allowed at the 90% CL. A pure D-wave decay is allowed for all values of cos φ. For positive cos φ a small S-wave partial width is allowed while for negative cos φ a large S-wave partial width is allowed. Similar conclusions were reached in the CLEO II study of the corresponding neutral states [8].

VIII. FRAGMENTATION

The momentum spectra for the decays, $D_2^*(2460)^+ \to D^0\pi^+$ and of $D_1(2420)^+ \to D^{*0}\pi^+$, were obtained by fitting the observed mass-difference spectra in five x_p bins from 0.5 to 1. Again, the masses and widths of both states were fixed to our measured values given above. For each x_p bin, the acceptance corrected yield is shown as the data points in Fig. 7 (a) and (b). The Peterson fragmentation function [17]:

$$\frac{dN}{dx_p} \propto \frac{1}{x_p[1 - \frac{1}{x_p} - \frac{\epsilon_p}{1-x_p}]^2}, \tag{3}$$

was fitted to the acceptance-corrected momentum spectra. This gave the values, $\epsilon_p = 0.020^{+0.011+0.003}_{-0.006-0.003}$ and $0.013^{+0.005+0.004}_{-0.005-0.004}$, respectively, for the $D_2^*(2460)^+$ and $D_1(2420)^+$ states. The results are shown in Fig. 7 (a) and (b). Both spectra are quite hard and are similar to those we obtained for both the $D_2^*(2460)^0$ and $D_1(2420)^0$ states [8] and for the $D_{s1}(2536)^+$ [18].

IX. CROSS SECTIONS TIMES BRANCHING RATIOS

Using the measured yields with the cos θ_π cut removed, the measured fragmentation functions to extrapolate to zero momentum, and after correcting for the efficiencies and the relevant D^0 and D^{*0} branching ratios, we have extracted the production cross sections times the branching ratios. The dependence on the D_J^+ alignment can be removed either by including events from the full range of cos θ_π or by selecting events with cos $\theta_\pi > 0$. We have listed in Table VI the weighted average of these two methods. In these calculations we have used the CLEO II measurements of the D^0 and D^{*0} branching ratios [19,20]. The systematic errors include the uncertainties in the branching ratios, the uncertainty from the differences between various fragmentation models (Peterson [17], Lund [21], and Kartvelishvili [22]), as well as the uncertainty in the extrapolation to $x_p = 0$.

The production cross sections times branching ratios for the D_J^+ states, given in Table VI, are similar to those measured in our earlier study of the D_J^0 states [8].

We also set the upper limit:

$$\frac{B[D_1(2420)^+ \to D^0\pi^+]}{B[D_1(2420)^+ \to D^{*0}\pi^+]} < 0.18 \text{ at } 90\% \text{ CL}. \tag{4}$$

For the $J^P = 1^+$ assignment for this state, this ratio must be zero.

Finally, we determined the ratio of the branching fractions:

$$\frac{B[D_2^*(2460)^+ \to D^0\pi^+]}{B[D_2^*(2460)^+ \to D^{*0}\pi^+]} = 1.9 \pm 1.1 \pm 0.3. \tag{5}$$

This result is consistent with the theoretical predictions discussed previously and with the ratio obtained in the earlier CLEO II study of the $D_2^*(2460)^0$ [8].

X. CONCLUSIONS

In conclusion, we have observed two charged charmed mesons with masses $2425 \pm 2 \pm 2$ MeV/c^2 and $2463 \pm 3 \pm 3$ MeV/c^2, and with widths 26^{+8+4}_{-7-4} MeV/c^2 and 27^{+11+5}_{-8-5} MeV/c^2 respectively. These have been identified as the probable isospin partners of the $D_1(2420)^0$ and the $D_2^*(2460)^0$, respectively. We determined the isospin mass splittings between the charged and neutral D_1 states to be 4^{+2+3}_{-3-3} MeV/c^2 and the corresponding value for the D_2^* states to be $-2 \pm 4 \pm 4$ MeV/c^2. The observed helicity angle distributions are in agreement with expectations for the decay of the $L = 1$ $D_1(2420)^+$ and $D_2^*(2460)^+$ states and are similar to those of their neutral partners. In addition, the measured widths of both charged states are consistent with the predictions for D-wave decays of these states. Still further support comes from the pattern in the decay channels for these states: regardless of the initial charge, the D_2^* decays both to $D\pi$ and to $D^*\pi$, while the D_1 decays to $D^*\pi$, but not to $D\pi$. Taken together, these results constitute strong evidence for identifying these two D_J^+ states as the charged $P_1^{(3/2)}$ and $P_2^{(3/2)}$ doublet predicted by HQET. This is the first definitive observation of the $D_1(2420)^+$ state and of the $D_2^*(2460)^+$ decay to $D^{*0}\pi^+$. For the $D_1(2420)^+ \to D^{*0}\pi^+$ decay, we obtain constraints on $\Gamma_S/(\Gamma_S+\Gamma_D)$ as a function of the cosine of the relative phase of the S-wave and D-wave amplitudes. We have also determined the production cross sections times branching ratios for the decay mode $D_1(2420)^+ \to D^{*0}\pi^+$, and for the two decay modes of $D_2^*(2460)^+ \to D^0\pi^+$ and $D^{*0}\pi^+$, obtaining values in good agreement with the corresponding values for the neutral states. In addition, we have set an upper limit for the decay $D_1(2420)^+ \to D^0\pi^+$. Lastly, we have extracted the ratio of the branching fractions for the decays $D_2^*(2460)^+ \to D^0\pi^+$ and $D_2^*(2460)^+ \to D^{*0}\pi^+$. This yielded a value of $1.9 \pm 1.1 \pm 0.3$ which is consistent both with theoretical expectations and with the corresponding result for the neutral state.

ACKNOWLEDGEMENTS

We gratefully acknowledge the effort of the CESR staff in providing us with excellent luminosity and running conditions. J.P.A., J.R.P., and I.P.J.S. thank the NYI program of the NSF, G.E. thanks the Heisenberg Foundation, I.P.J.S. and T.S. thank the TNRLC, K.K.G., M.S., H.N.N., T.S., and H.Y. thank the OJI program of DOE, J.R.P thanks the A.P. Sloan Foundation, S.M.S. thanks the Islamic Development Bank, and A.W. thanks the Alexander von Humboldt Stiftung for support. This work was supported by the National Science Foundation, the U.S. Dept. of Energy and the Natural Sciences and Engineering Research Council of Canada.

REFERENCES

[1] Particle Data Group, L. Montanet et al., Phys. Rev. D 50, (1994).
[2] ARGUS Collab., H. Albrecht et al., Phys. Rev. Lett. 56, 549 (1986).
[3] ARGUS Collab., H. Albrecht et al., Phys. Lett. B 221, 422 (1989).
[4] ARGUS Collab., H. Albrecht et al., Phys. Lett. B 232, 398 (1989).
[5] E691 Collab., J.C. Anjos et al., Phys. Rev. Lett. 62, 1717 (1989).
[6] CLEO Collab., P. Avery et al., Phys. Rev. D 41, 774 (1990).
[7] E687 Collab., P.L. Frabetti et al., Phys. Rev. Lett. 72, 324 (1994).
[8] CLEO Collab., P. Avery et al., Phys. Lett. B 331, 236 (1994).
[9] ARGUS Collab., H. Albrecht et al., Phys. Lett. B 231, 208 (1989).
[10] N. Isgur and M.B. Wise, Phys. Rev. Lett. 66, 1130 (1991).
[11] M. Lu, M. Wise and N. Isgur, Phys. Rev. D 45, 1553 (1992).
[12] J. L. Rosner, Comm. Nucl. Part. Phys. 16, 109 (1986).
[13] S. Godfrey and R. Kokoski, Phys. Rev. D 43, 1679 (1991).
[14] A. F. Falk and M. E. Peskin, Phys. Rev. D 49, 3320 (1994).
[15] CLEO Collab., Y. Kubota et al., Nucl. Inst. Meth. A320, 66 (1992).
[16] S. Godfrey and N. Isgur, Phys. Rev. D 32, 189 (1985).
[17] C. Peterson et al., Phys. Rev. D 27, 105 (1983).
[18] CLEO Collab., J.P. Alexander et al., Phys. Lett. B 303, 377 (1993).
[19] CLEO Collab., D.S. Akerib et al., Phys. Rev. Lett. 71, 3070 (1993).
[20] CLEO Collab., F. Butler at al., Phys. Rev. Lett. 69, 2041 (1992).
[21] B. Andersson et al., Phys. Rep. 97, 31 (1983).
[22] V.G. Kartvelishvili et al., Phys. Lett. B 78, 615 (1978).

TABLES

TABLE I. Allowed strong decays of D_J to $D\pi$ and $D^*\pi$ in the $m_Q \to \infty$ limit. L_f is the orbital angular momentum between the decay products.

State ($L_J^{(j)}$)	J^P	$D\pi$	$D^*\pi$
$P_2^{(3/2)}$	2^+	$L_f = 2$	$L_f = 2$
$P_1^{(3/2)}$	1^+	-	$L_f = 2$
$P_1^{(1/2)}$	1^+	-	$L_f = 0$
$P_0^{(1/2)}$	0^+	$L_f = 0$	-

TABLE II. The $D_2^*(2460)^+$ mass and width in MeV/c^2.

Experiment	Mass	Width
CLEO II	$2463 \pm 3 \pm 3$	$27^{+11+5}_{-\ 8-5}$
ARGUS [9]	$2469 \pm 4 \pm 6$	$14 \pm 5 \pm 8$
E687 [7]	$2453 \pm 3 \pm 2$	$23 \pm 10 \pm 5$

TABLE III. The D_2^* and D_1 isospin mass splittings in MeV/c^2.

Experiment	$M[D_2^*(2460)^+] - M[D_2^*(2460)^0]$	$M[D_1(2420)^+] - M[D_1(2420)^0]$
CLEO II	$-2 \pm 4 \pm 4$	4^{+2+3}_{-3-3}
ARGUS [9]	$14 \pm 5 \pm 8$	
E691 [5]		$15 \pm 11 \pm 7$ [§]
E687 [7]	$0 \pm 4 \pm 3$	

[§] This value was derived from results presented in ref. [5], the errors having been added in quadrature.

TABLE IV. List of spin-parity hypotheses and the corresponding helicity angle distributions. $A_{\lambda 0}$ is the amplitude to produce a D^* with helicity λ.

Spin-Parity Hypothesis	Angular Distribution
0^+	forbidden
0^-	$\cos^2\alpha$
$1^-, 2^+, 3^-, \ldots$	$\sin^2\alpha$
$1^+, 2^-, 3^+, \ldots$	$\lvert A_{10}\rvert^2 \sin^2\alpha + \lvert A_{00}\rvert^2 \cos^2\alpha$

TABLE V. χ^2 and CL for various helicity angle distributions.

State	Angular Distribution	χ^2/N_{dof}	CL
$D_2^*(2460)^+$	$\sin^2\alpha$	1.3/3	72.9%
	isotropic	6.1/3	10.7%
	$\cos^2\alpha$	29.2/3	2.0×10^{-6}
$D_1(2420)^+$	$1 + 3\cos^2\alpha$	1.7/3	63.7%
	$\cos^2\alpha$	6.7/3	8.2%
	isotropic	8.7/3	3.4%
	$\sin^2\alpha$	27.8/3	4.0×10^{-6}

TABLE VI. Production cross sections times branching ratios (pb).

Decay Mode	$\sigma(e^+e^- \to D_J^+ X) \cdot B(D_J^+)$
$D_2^*(2460)^+ \to D^0\pi^+$	$21.9 \pm 7.7 \pm 2.3$
$D_2^*(2460)^+ \to D^{*0}\pi^+$	$11.5 \pm 5.1 \pm 1.4$
$D_1(2420)^+ \to D^{*0}\pi^+$	$26.4 \pm 7.1 \pm 2.8$

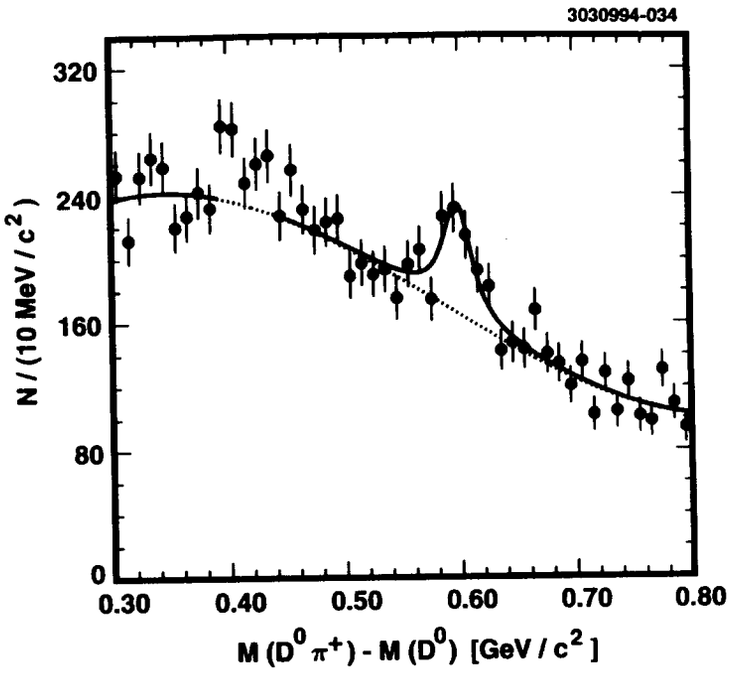

FIG. 1. The $M(D^0\pi^+) - M(D^0)$ mass-difference distribution for $P_{tot} > 0.1$, as described in the text. The solid line shows the complete fit while the dashed line shows the background contribution.

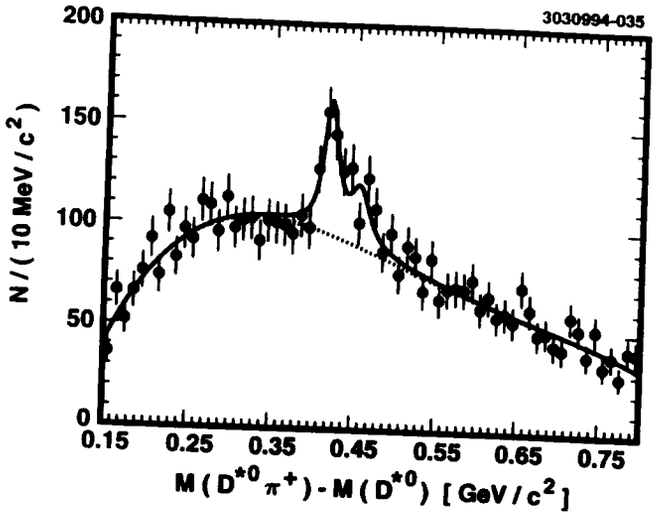

FIG. 2. The $M(D^{*0}\pi^+) - M(D^{*0})$ mass-difference distribution for $-1 \leq \cos\alpha \leq +1$, as described in the text. The solid line shows the complete fit while the dashed line shows the background contribution.

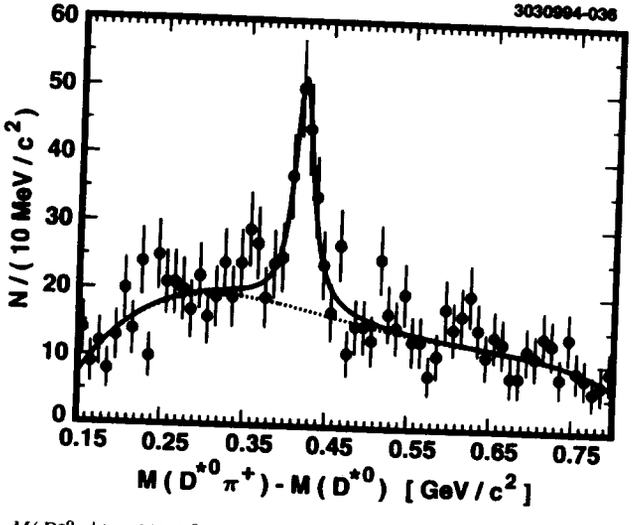

FIG. 3. The $M(D^{*0}\pi^+) - M(D^{*0})$ mass-difference distribution for $|\cos\alpha| > 0.8$, as described in the text. The solid line shows the complete fit while the dashed line shows the background contribution.

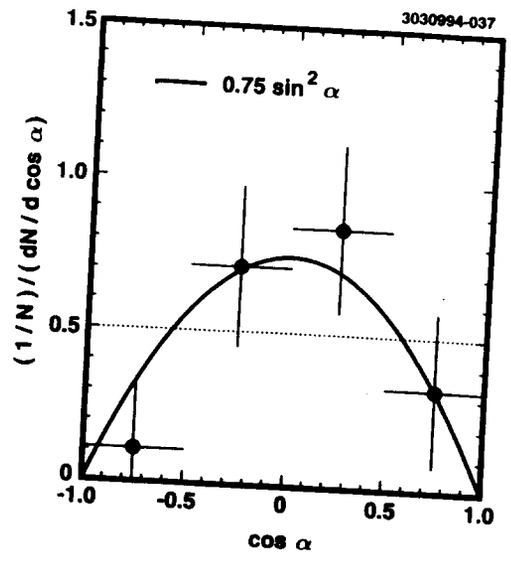

FIG. 4. The normalized helicity angle distribution for the $D_2^*(2460)^+$, as described in the text.

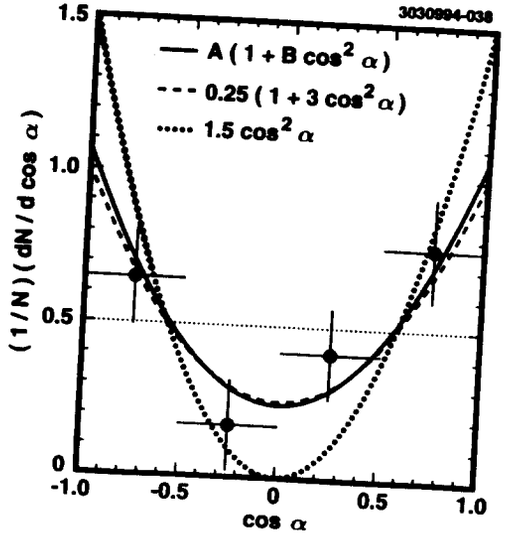

FIG. 5. The normalized helicity angle distribution for the $D_1(2420)^+$, as described in the text.

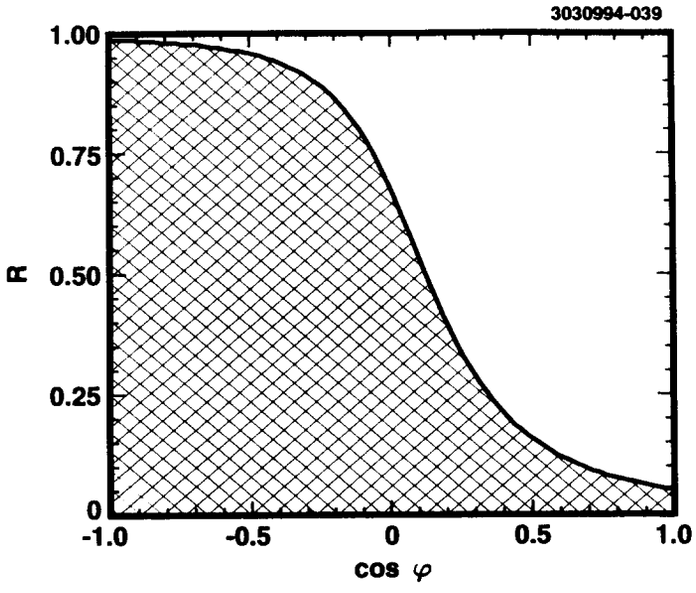

FIG. 6. Plot of R = $\Gamma_S/(\Gamma_S+\Gamma_D)$ versus cosine of the relative phase of S and D wave amplitudes in the $D_1(2420)^+ \to D^{*0}\pi^+$ decay. The hatched area represents the 90% confidence level allowed region.

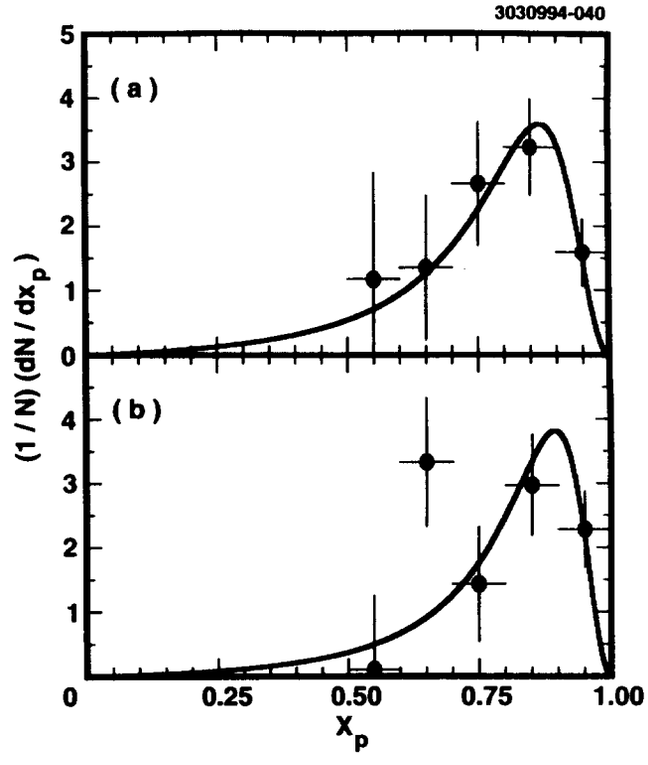

FIG. 7. The momentum spectra of (a) $D_2^*(2460)^+ \to D^0\pi^+$ and (b) $D_1(2420)^+ \to D^{*0}\pi^+$. The solid lines show results of fitting the Peterson fragmentation function to the data.